International Journal of Computer Information Systems and Industrial Management Applications
ISSN 2150-7988 Volume 18(9s) 2026 pp. 287-304
https://doi.org/10.70917/ijcisim-2026-3441
Article

COMPARATIVE EVALUATION OF PERVAPORATION MEMBRANES FOR SUSTAINABLE INDUSTRIAL DMC DEHYDRATION: PROCESS PERFORMANCE AND SELECTION CRITERIA

Arvind S Madalgi[1], Swapna Rekha Panda[*1], Haresh K Dave[2], Kaushik Nath[2]

[*1]Department of Chemical Engineering, Shroff S. R. Rotary Institute of Chemical Technology, UPL University of Sustainable Technology, Block No: 402, 393135, Gujarat, India.
[2]Department of Chemical Engineering, G H Patel College of Engineering & Technology, The Charutar Vidya Mandal (CVM) University, Vallabh Vidyanagar –388120, Gujarat, India.

Corresponding author: [*1]Swapna Rekha Panda
swapna.rekha@gmail.com
ORCID Id: https://orcid.org/0000-0003-0755-5829

Abstract: Revised: Solvent dehydration remains a critical unit operation in industrial purification, where membrane-based separations can offer an energy-efficient alternative to conventional distillation. This study presents a comparative evaluation of two commercial pervaporation membranes for the dehydration of an industrial dimethyl carbonate (DMC)/water feed obtained from a distillation-based process in Cycle 1. Performance was assessed under varying temperature and feed-composition conditions using total flux, separation factor, water permeability, membrane selectivity, pervaporation separation index, and Arrhenius-based transport parameters in Cycle 2. Among the membranes tested, PERVAP® 4100 showed the highest selectivity, reaching a separation factor of 2852 at 35 °C with 90 wt% DMC, whereas Plasma 2540 showed lower selectivity but higher water permeability under identical conditions. Temperature increased the permeation flux of both membranes, while higher DMC concentrations improved selectivity but reduced water flux. Characterization by FTIR, TGA, contact-angle analysis, and mechanical testing was used to relate membrane structure to separation performance. Intrinsic membrane performance parameters including water permeability (Pw), membrane selectivity (αmem), diffusivity (Dw), and activation energy of permeation (Ep) using the Arrhenius framework using both the commercial membranes are reported in our study. PERVAP 4100 showed much higher selectivity (separation factor of up to 2852 at 35 C 90 wt% DMC) than Plasma 2540 (132.85 under the same conditions), whilst Plasma 2540 was found to be more water permeable (Pw up to 1.64×10^{-12} barrer). The results provide a comparative basis for selecting commercial membranes for industrial DMC dehydration and for designing more efficient solvent-purification workflows.
Keywords: Pervaporation; Dimethyl Carbonate; Industrial Effluent; Membrane Dehydration; Separation Factor.

1. INTRODUCTION

Dimethyl carbonate (DMC, $C_3H_6O_3$; MW = 90.08 g/mol; bp = 90.3°C) has risen to prominence as a multifunctional green solvent, methylating agent, electrolyte co-solvent in lithium-ion batteries, and sustainable substitute for hazardous chloromethylation and phosgenation agents in organic synthesis. Its low acute toxicity, facile biodegradability, and high polarity index (combined with moderate H-bonding capacity) position it as an industrially strategic solvent within the framework of green chemistry principles [1, 2]. DMC is miscible with most organic solvents and is slightly soluble in water (up to ~13 wt% at 20°C), a property that presents significant purification

challenges. The recovery and purification of DMC from its industrial effluent streams particularly the removal of residual water to achieve anhydrous or near-anhydrous grades constitutes a critical and challenging unit operation. The binary DMC/water system exhibits a narrow miscibility window: homogeneous mixtures occur only at DMC concentrations below approximately 15 wt% or above approximately 97 wt%, with a liquid-liquid immiscibility region in between [3]. Dimethyl carbonate (DMC) is an important industrial solvent, and efficient removal of water is essential for improving product quality and process sustainability. This study evaluates the pervaporation performance of two commercial membranes for dehydrating an industrial DMC/water mixture and compares their separation behavior under different operating conditions.

Furthermore, DMC and water form a minimum-boiling azeotrope at 77.5°C with approximately 11 wt% water, rendering conventional fractional distillation ineffective for producing high-purity anhydrous DMC [4, 5]. Pervaporation (PV) offers an elegant and energy-efficient alternative to distillation-based dehydration, particularly for azeotropic and thermally sensitive systems. In pervaporation, a liquid feed mixture contacts one face of a dense polymeric membrane; selective sorption and diffusion of one component in this case, water through the membrane matrix under a vacuum-maintained chemical potential gradient results in preferential permeation. The separation is governed by the solution-diffusion model, with molecular transport dictated by the sorption coefficient and diffusivity of each component in the membrane polymer [6, 7]. Poly(vinyl alcohol) (PVA) remains the benchmark polymer for hydrophilic pervaporation membranes. Its abundance of hydroxyl groups imparts high intrinsic affinity for water, excellent film-forming properties, and tunable selectivity through chemical or physical cross-linking (Bolto et al., 2009; Svang-Ariyaskul et al., 2006). The degree and type of cross-linking critically determine the permeability-selectivity trade-off: highly cross-linked PVA membranes exhibit reduced chain mobility and matrix swelling, yielding superior selectivity at the expense of some permeation flux. Composite PVA membranes deposited on porous poly(acrylonitrile) (PAN) support layers have become the industrial standard, balancing mechanical robustness with high water-selective transport [8, 9]. A scant work is being published in the literarture in the Pervaporative dehydration of DMC -water (<1% moisture content). We have identified two commercial membranes for the Pervaporative dehydration of DMC/Water mixture. This work deals with the two such commercial PVA/PAN composite membranes within the context of a Cycle 2 industrial DMC recovery process. The feed stream sourced from a distillation-based DMC recovery column typically contains approximately 93 wt% DMC, less than 5 wt% water, and approximately 2 wt% other organic impurities. The dehydration target by the is a product containing greater than 99 wt% DMC and less than 1 wt% water. The membranes under investigation are PERVAP™ 4100 (DeltaMem AG, Switzerland) and Plasma 2540 (Shivohm Membrane Systems, Sangli, India), both PVA/PAN composites having differing in cross-linking degree, selective layer geometry, and support structure. The specific objectives of this study are to: (i) systematically investigate the effects of feed temperature (35–65 °C) and feed DMC concentration (90–97.5 wt%) on the total permeation flux, separation factor, component fluxes, and pervaporation separation index (PSI) of PERVAP™ 4100 and Plasma 2540 membranes; (ii) determine the intrinsic membrane transport parameters, including water permeability (Pw), membrane selectivity (αmem), water diffusivity (Dw), and activation energy of permeation (Ep), using the Arrhenius framework; (iii) quantify the swelling behaviour of both membranes in DMC/water mixtures of varying compositions and correlate it with membrane separation performance; (iv) establish structure–performance relationships through comprehensive membrane characterization; and (v) evaluate the industrial suitability of both commercial membranes for second-cycle DMC dehydration and provide quantitative guidance for membrane selection.

2. PERVAPORATION FUNDAMENTALS AND TRANSPORT THEORY

The theoretical framework for pervaporation transport in dense polymeric membranes is most accurately described by the solution-diffusion model, first rigorously articulated by Paul and Yampol'skii [11] and elaborated by Wijmans and Baker [12]. In this model, transport occurs in three sequential steps: (i) sorption of feed components from the liquid feed into the membrane at the upstream interface, (ii) diffusion of sorbed molecules through the membrane polymer under a chemical potential gradient, and (iii) desorption into the vapor phase at the low-pressure downstream face. The chemical potential gradient is maintained by applying a vacuum or sweep gas on the permeate side, creating a partial pressure differential for each permeating component. Membrane permeability (P) is the product of the sorption coefficient (S) and the diffusivity (D): $P = S \times D$. Selectivity arises from differential sorption (ΔS) or differential diffusivity (ΔD) or both. For hydrophilic PVA-based membranes separating water/organic azeotropes, the dominant contribution to water selectivity is the preferential sorption of water (high Sw) combined with the large size difference between water (kinetic diameter 0.265 nm) and DMC (0.47 - 0.63 nm), which suppresses DMC diffusivity through the cross-linked polymer network [13,14]. The plasticization phenomenon whereby absorbed water molecules disrupt inter-chain hydrogen bonding and increase segmental chain mobility is a critical process governing the

permeability-selectivity trade-off in PVA membranes. Cross-linking constrains this chain mobility, reducing swelling and maintaining selectivity under high-water-activity feed conditions [15,16].

2.1 PVA-Based Membranes for Organic Solvent Dehydration

Poly(vinyl alcohol) membranes have been intensively studied for pervaporative dehydration of ethanol/water, isopropanol/water, acetone/water, and DMC/water systems. The seminal work of Huang [17] established PVA as the benchmark hydrophilic membrane material. Subsequent cross-linking studies using glutaraldehyde (GA), maleic acid, and tetraethyl orthosilicate (TEOS) demonstrated that the degree of cross-linking is the most critical parameter determining the selectivity-permeability balance [18,19]. Won et al. [20] investigated pervaporation of DMC/methanol/water mixtures using chitosan membranes and highlighted the unusual negative temperature dependence of water activity in DMC-rich solutions a key thermodynamic feature that distinguishes DMC/water PV from other systems. Kang et al. [10] systematically evaluated cross-linked PVA membranes for DMC dehydration across a wide composition range, reporting separation factors of 200 - 800 at 50°C in the 90 - 97 wt% DMC range. Dogan and Hilmioglu [21] demonstrated the influence of crosslinker concentration on PVA membrane structure and found an optimal cross-linking density that balanced flux and selectivity. Tang et al. [22] studied PVA/silica hybrid membranes for DMC dehydration and reported improved thermal stability and selectivity with addition of functionalized silica nanoparticles. Commercial PVA/PAN composite membranes, particularly the PERVAP™ series (formerly GFT, now DeltaMem AG), have been benchmark products in industrial pervaporation since the 1980s. Neel [23] reviewed early commercial applications and noted the importance of the PAN support layer morphology in determining mass transfer resistance, a finding consistent with the broader literature on PAN ultrafiltration support fabrication via phase inversion [24]. Liu et al. [25] characterized the pore structure of PAN support membranes and reported that a finger-like macrovoid morphology minimizes support-layer resistance. Zhang et al. [26] compared several commercial PVA-based dehydration membranes and found that thinner selective layers (< 3 µm) consistently delivered higher fluxes with comparable selectivity to thicker counterparts. Beyond conventional cross-linked PVA, recent work has explored zeolite-filled and nanostructured fillers to push the permeability-selectivity trade-off further, including ultrathin zeolite X membranes for ethanol dehydration [27] and graphene oxide-carbon nanotube hybrid mixed matrix membranes that combine hydrophilic transport pathways with mechanical reinforcement [28]. Metal-organic framework modifiers, such as Zr-based MOFs incorporated into PVA matrices, have likewise been reported to enhance pervaporation selectivity for alcohol dehydration while retaining the PAN-supported composite architecture used industrially [29].

2.2 Effect of Operating Parameters on Pervaporation Performance

The influence of feed temperature on pervaporation flux follows Arrhenius-type behavior: $J = J_0 \exp(-Ep/RT)$, where Ep is the apparent activation energy of permeation, R is the universal gas constant, and T is the absolute temperature [30]. Higher temperatures increase diffusion coefficients and reduce feed viscosity, typically enhancing flux. However, elevated temperatures also reduce membrane selectivity through accelerated plasticization and increased DMC co-permeation [31]. For the DMC/water system specifically, the complex phase behavior including the negative temperature dependence of water activity in DMC-rich mixtures [20] creates a non-trivial competition between thermodynamic driving force reduction and diffusional enhancement. Feed composition strongly influences PV performance through its effect on membrane swelling. As water content in the feed increases, the driving force for water permeation and membrane swelling both increase, leading to higher flux but reduced selectivity [32]. At high DMC concentrations (> 95 wt%), water activity is low, minimizing swelling and yielding the highest selectivity but lowest flux. This underscores the importance of characterizing membrane performance across the full industrially relevant concentration range [33]. Permeate pressure affects the driving force by modifying the activity of permeating species at the downstream membrane face. At permeate pressures below the saturation vapor pressure of the more permeable component (water), the effect is negligible; above this threshold, permeate pressure resistance reduces effective driving force and flux (Wijmans and Baker, 1995). In this study, a downstream pressure of 30 mmHg was maintained, well below the saturation vapor pressure of water at all studied temperatures.

3. MATERIALS AND METHODS

3.1 Feed Materials

Binary DMC/water feed mixtures were prepared by combining analytical-grade dimethyl carbonate (purity ≥99.5 wt%; sourced from Chem-Lab Analytical, Belgium, and Thommen-Furler AG, Switzerland) with deionized distilled water (conductivity < 1 µS/cm). Four feed compositions were prepared gravimetrically to contain 90, 92.5,

95, and 97.5 wt% DMC (corresponding to 10, 7.5, 5, and 2.5 wt% water, respectively), spanning the industrially relevant range for Cycle 2 dehydration. All feed mixtures were verified by Karl Fischer coulometric titration (Metrohm 851 Titrando) prior to each experimental run, with moisture values confirmed within ±0.05 wt% of target composition.

3.2 Commercial Membranes

Two commercial hydrophilic composite membranes were evaluated in this study, i.e., PERVAP™ 4100 (DeltaMem AG, Switzerland). A three-layer composite structure comprising a dense, highly cross-linked PVA selective layer (2 - 3 µm thick), cast on a porous PAN support membrane (30 µm thick; average surface pore size 20 nm), laminated onto a polyester non-woven fabric backing (80 - 120 µm). The selective layer is prepared by knife-coating a concentrated PVA solution onto the PAN support followed by thermal and chemical cross-linking treatment. This membrane is designed specifically for high-selectivity dehydration of organic solvents at low water concentrations. Plasma 2540 (Shivohm Membrane Systems, Sangli, Maharashtra, India): A composite PVA/PAN membrane with a PVA selective layer of approximately 3 µm, a PAN porous support of approximately 80 µm, and a polyester non-woven fabric backing (~100 µm). The membrane undergoes moderate cross-linking relative to PERVAP™ 4100, resulting in a higher baseline water permeability but lower selectivity. The Plasma 2540 is positioned as a cost-effective option for industrial solvent dehydration applications. Table 1 discuss the structural and characterization properties of PERVAPTM 4100 and PLASMA 2540 membranes.

Table 1 Structural properties of PERVAP™ 4100 and Plasma 2540 membranes

Property	**PERVAP™ 4100**	**Plasma 2540**	**Reference**
Membrane Type	Composite hydrophilic pervaporation membrane	Composite hydrophilic pervaporation membrane	[34,35]
Selective Layer Material	Cross-linked Poly(vinyl alcohol) (PVA)	Cross-linked Poly(vinyl alcohol) (PVA)	[25,30]
Selective Layer Thickness (µm)	2–3	~3	[34,35]
Support Layer	Polyacrylonitrile (PAN)	Polyacrylonitrile (PAN)	[30,34,35]
Backing Layer	Polyester Non-Woven Fabric (PET NWF)	Polyester Non-Woven Fabric (PET NWF)	[34,35]
Separation Mechanism	Solution–Diffusion	Solution–Diffusion	[11,12]
Membrane Hydrophilicity	Hydrophilic	Hydrophilic	[13]
Typical Application	Dehydration of organic solvents	Dehydration of organic solvents	[16,34,35]
Operating Temperature Range (°C)	30 - 90	30 - 90	[34,35]
Membrane Geometry	Flat-sheet Composite	Flat-sheet Composite	[34,35]
Transport Model	Solution - Diffusion	Solution - Diffusion	[12]

3.3 Pervaporation Experimental Setup

Pervaporation experiments were carried out using a stainless-steel flat-sheet membrane cell with an effective membrane area of 160 cm². The experimental apparatus comprised a feed recirculation circuit driven by a peristaltic pump, a thermostatically controlled water bath (Julabo F25-MC, ±0.1°C accuracy), and a vacuum pump maintaining downstream pressure at full vaccum, monitored by a digital pressure transducer. The permeate vapors were collected in cold traps immersed in liquid nitrogen. A schematic of the experimental setup is presented in Fig. 1.

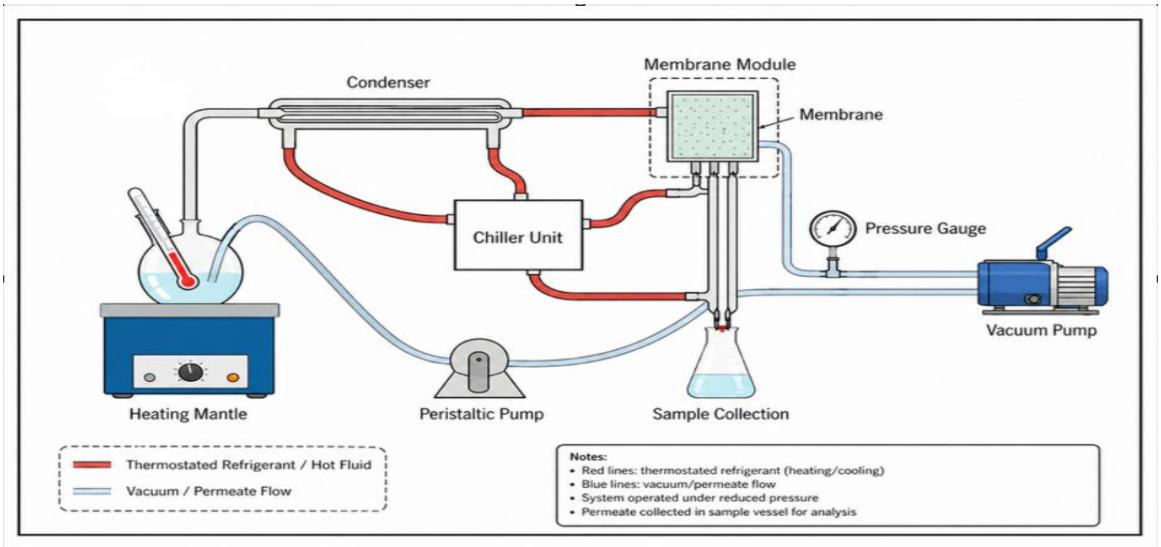

Fig. 1 Schematic diagram of the pervaporation experimental setup

Two litres of feed solution were circulated continuously across the membrane surface. The system was allowed to equilibrate for 1.0 - 1.5 hours prior to permeate collection. Permeate fractions were collected gravimetrically (Mettler Toledo XP205 analytical balance, ±0.01 mg) over a measured time interval. Each experiment was repeated twice using freshly prepared feed solutions, and averaged results are reported. Feed and permeate compositions were analysed by Karl Fischer titration (Metrohm 851 Titrando). For ease of presentation and comparison of experimental results, the commercial membranes investigated in this study were assigned identification codes. These codes were used consistently throughout the mechanical characterization, thermal analysis, and pervaporation performance evaluation sections.

Table 2 Coding scheme for the commercial membranes used in the study

Code	Membrane
H1	PERVAP™ 4100
H2	Plasma 2540

Table 2 discuss the coding system adopted solely for graphical representation and statistical comparison of membrane properties. H1 corresponds to the commercial PERVAP™ 4100 membrane supplied by DeltaMem AG (Switzerland), while H2 represents the Plasma 2540 membrane supplied by Shivohm Membrane Systems (India).

3.4 Performance Parameters

Pervaporation performance was characterized using the following parameters:

Total Permeation Flux (J)

$$J = \frac{m}{(A \times t)} \quad (1)$$

where m is permeate mass (kg), A is effective membrane area (m^2), t is collection time (s). Units: kg m^{-2} s^{-1}.

Component Flux (J_i)

$$J_i = \frac{m_i}{(A \times t)} \quad (2)$$

where m_i is the mass of component i in the permeate.

Separation Factor (α)

$$\alpha = \frac{\left(\frac{Y_i}{Y_j}\right)}{\left(\frac{X_i}{X_j}\right)} \quad (3)$$

where Y_i and X_i are weight fractions of water (i) and DMC (j) in the permeate and feed, respectively.

Water Permeability (Pw)

$$Pw = \frac{(Jw \times l)}{(x_i \times \gamma_i \times p_i,\ sat - p_p)} \quad (4)$$

reported in barrer (1 barrer = 10^{-10} cm³(STP)·cm / cm²·s·cmHg), where l is selective layer thickness, γ_i the activity coefficient, p_i, sat the saturated vapor pressure, and p_p the permeate pressure (neglected due to low value).

Membrane Selectivity (αmem)

$$\alpha mem = \frac{Pw}{P_{DMC}} \quad (5)$$

The intrinsic selectivity independent of driving force conditions.

Pervaporation Separation Index (PSI)

$$PSI = J \times (\alpha - 1) \quad (6)$$

An integrated performance metric balancing flux and selectivity.

Degree of Swelling (%)

Percentage degree of swelling was determined as [17]. Membrane samples are cut, dried to constant weight (W_0), then immersed in water or water–organic mixtures at a fixed temperature until equilibrium. After surface blotting, the swollen weight (W_s) is measured.

Degree of swelling (%) is calculated as,

$$Swelling\ (\%) = \frac{W_s - W_0}{W_0} \times 100 \quad (7)$$

This quantifies water uptake and polymer chain relaxation, directly reflecting membrane stability during dehydration.

Activation Energy of Permeation (Ep)

$$ln\ ln\ (J) = ln\ ln\ (J^0) - \frac{Ep}{(RT)} \quad (8)$$

where J_0 is the pre-exponential factor, R = 8.314 J mol^{-1} K^{-1}, and T is absolute temperature. E_p is obtained from the slope of ln(J) vs. 1/T plots.

3.5 Membrane Characterization

3.5.1 FTIR Spectroscopy

ATR-FTIR spectra were recorded on a Bruker Tensor 27 FTIR spectrometer over 600 - 4000 cm^{-1} at 4 cm^{-1} resolution (64 scans averaged). Spectra are presented in Fig. 2.

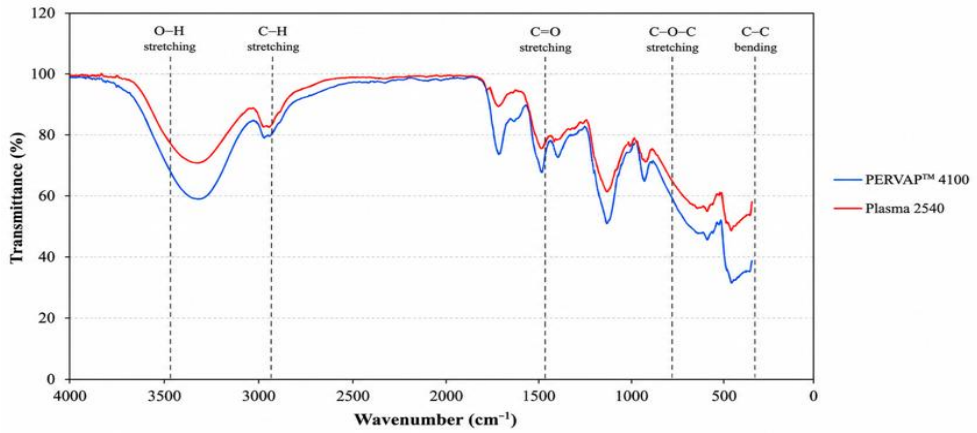

Fig. 2 FTIR spectra of PVA/PAN composite membranes

FTIR spectra of both membranes (Fig. 2) confirmed the characteristic functional groups of PVA-based composite membranes. A broad O–H stretching band at 3200–3600 cm^{-1} was observed in both membranes, corresponding to the hydroxyl groups of the PVA selective layer. C–H stretching bands appeared at approximately 2910–2940 cm^{-1}, while absorption peaks at around 1735 cm^{-1} and within the 1000–1200 cm^{-1} region were assigned to C=O and C–O–C stretching vibrations, respectively. The principal difference between the membranes was the intensity of the C–O–C stretching band near 1021 cm^{-1}, which is associated with acetal linkages formed during PVA cross-linking [18], consistent with the characteristic acetal-bridge absorptions reported for glutaraldehyde-crosslinked PVA hydrogels [36] and with acid-catalysed crosslinking studies linking C–O–C band intensity directly to crosslink density [37]. PERVAP™ 4100 exhibited a stronger C–O–C absorption, indicating a higher degree of chemical cross-linking than Plasma 2540. In contrast, Plasma 2540 showed a relatively stronger O–H stretching band, suggesting a greater concentration of residual hydroxyl groups. These findings indicate that PERVAP™ 4100 possesses a more extensively cross-linked structure, which is expected to reduce swelling and enhance separation selectivity, consistent with previous studies on cross-linked PVA membranes [33].

3.5.2 Contact Angle Measurement

Static water contact angles were measured using a CAM 110-O4W goniometer (KSV Instruments, Taiwan) equipped with a CCD camera, consistent with the sessile-drop methodology widely used to evaluate membrane surface wettability and hydrophilicity [38]. Sessile drops of deionized water (2 µL) were placed on dry membrane surfaces and contact angles recorded after 5 seconds of equilibration. Results are the average of five measurements at different surface locations. Contact angle comparison is presented in Fig. 3

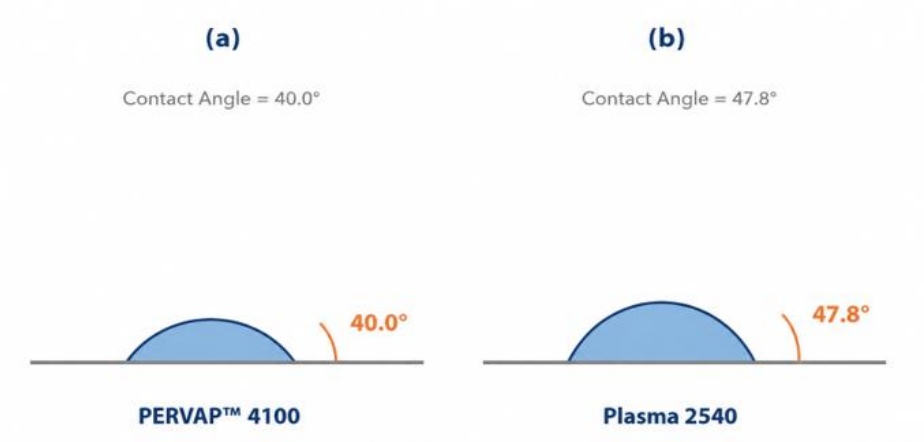

Fig. 3 Water contact angle (a) PERVAP™ 4100 (38 - 42°) (b) Plasma 2540 (43-47.8°)

Fig. 3 illustrates the water contact angle of the PERVAP™ 4100 membrane and Plasma 2540 membranes exhibited a contact angle of 40.0°±5 and 47.8°±5, indicating high hydrophilicity and strong affinity towards water indicating surface wettability because of surface chemistry and energy.

3.5.3 Thermogravimetric Analysis (TGA)

TGA data (Fig. 4) confirmed the thermal resilience of both membranes well above the operating temperature range of 35 - 65°C. PERVAP™ 4100 showed a T(5%) of 332°C and T(10%) of 362.5°C, with a residual mass at 400°C (R400) of 32.2 wt%. Plasma 2540 exhibited a slightly lower T(5%) of 329.7°C and T(10%) of 353.7°C, but a substantially higher R400 of 59.33 wt%. The higher char yield of Plasma 2540 at 400°C may reflect the contribution of its thicker PAN support layer (PAN degrades more slowly and leaves a higher carbon residue than PVA, consistent with the phase-inversion-cast PAN ultrafiltration support morphologies described by [24]) or the presence of surface treatment agents. The lower residue of PERVAP™ 4100 is consistent with a more extensive thermal decomposition of a densely cross-linked PVA network, which undergoes a sharper, more complete oxidative degradation above its decomposition onset, a pattern also reported for sol-gel PVA/silica hybrid membranes where increased cross-linking density correlates with sharper thermal decomposition profiles [39,40]. Both membranes are confirmed thermally stable for the studied operating conditions, consistent with literature values for cross-linked PVA [13,15].

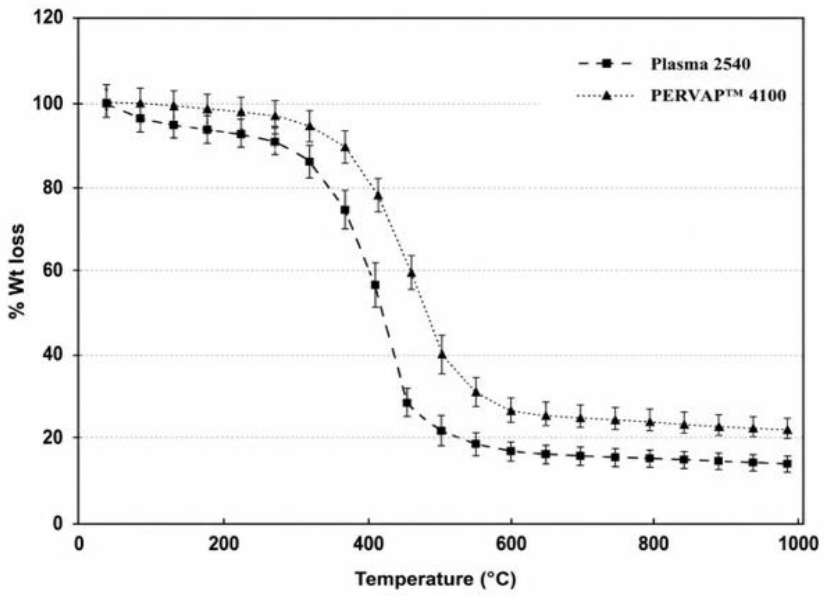

Fig. 4 Thermogravimetric analysis (TGA) profiles of PVA/PAN composite membranes

3.5.4 Mechanical Testing

PERVAP™ 4100 demonstrated significantly superior mechanical properties compared to Plasma 2540. Its tensile strength of 50 N/mm² and elongation at break of 45% reflect the structural benefits of its dense, highly cross-linked PVA network combined with the robust polyester NWF backing. These attributes are critical for sustained operation under continuous vacuum conditions in an industrial setting, where membrane creep and fatigue under differential pressure represent real failure modes [16]. Plasma 2540 exhibited a tensile strength of only 17.5 N/mm² and elongation at break of 30%, indicating a more brittle character relative to PERVAP™ 4100. This reduced mechanical robustness is consistent with its lower cross-linking degree and may restrict its operational pressure window. However, for the moderate vacuum conditions (30 mmHg downstream) employed in this study, both membranes demonstrated adequate mechanical integrity throughout all experimental runs without evidence of deformation or failure.

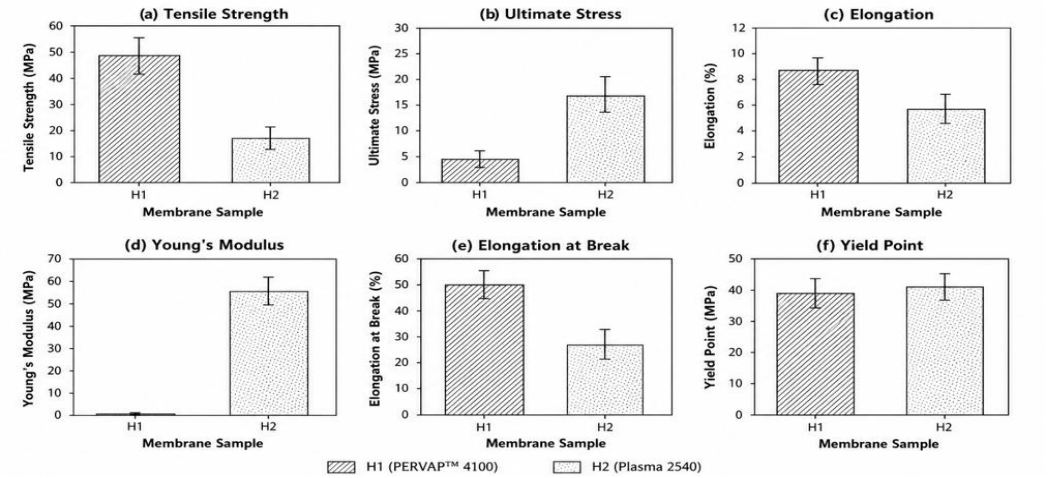

Fig. 5 Mechanical Properties of the Membranes

Figure 5 compares the mechanical properties of the pristine PERVAP™ 4100 (H1) membrane with the Plasma 2540-treated (H2) membrane. Plasma treatment resulted in a significant decrease in tensile strength and elongation, indicating reduced flexibility after surface modification and tuned composition. In contrast, the ultimate stress and Young's modulus increased markedly, demonstrating enhanced stiffness and resistance to deformation. The yield point remained nearly unchanged, suggesting that the onset of permanent deformation was minimally affected. These findings indicate that plasma treatment improved the membrane's structural rigidity and mechanical stability while reducing its ductility, making the modified membrane suitable for demanding pervaporation operating conditions.

3.5.5 Swelling Index

The swelling index of both membranes increased progressively with increasing water content in the DMC/water mixture, indicating greater solvent uptake at higher water concentrations. The Plasma 2540-treated membrane exhibited consistently higher swelling than the pristine PERVAP™ 4100 membrane across all compositions, reaching approximately 45% at 100 wt% water compared to 30% for the untreated membrane. This enhanced swelling suggests that plasma treatment increased the membrane's affinity for water by modifying its surface characteristics. Although swelling increased, the controlled behaviour indicates improved hydrophilic interaction, which can facilitate water transport while maintaining sufficient structural integrity for efficient pervaporation performance.

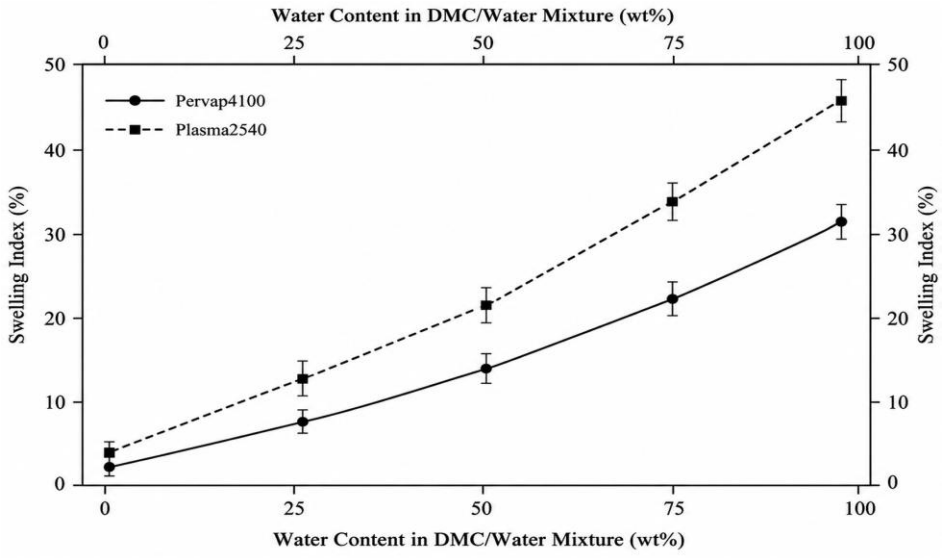

Fig. 6 Swelling Index Comparison

This stark difference in swelling behaviour is a direct consequence of the difference in cross-linking density. Higher cross-linking in PERVAP™ 4100 creates a tighter network that physically restricts chain mobility and water uptake, maintaining dimensional stability and selectivity even at high water activities. Conversely, the less cross-linked PVA network of Plasma 2540 absorbs more water, increasing polymer free volume and chain mobility which explains its higher water permeability but lower selectivity. Both membranes showed minimal swelling in pure DMC (≤ 6.8%), confirming that DMC sorption is not a primary cause of performance variation. These findings are consistent with swelling studies on cross-linked PVA membranes reported in the literature [18, 31, 32].

4. RESULTS AND DISCUSSION

4.1 Pervaporation Performance

4.1.1 Effect of Temperature and Feed Composition on Total Flux and Separation Factor

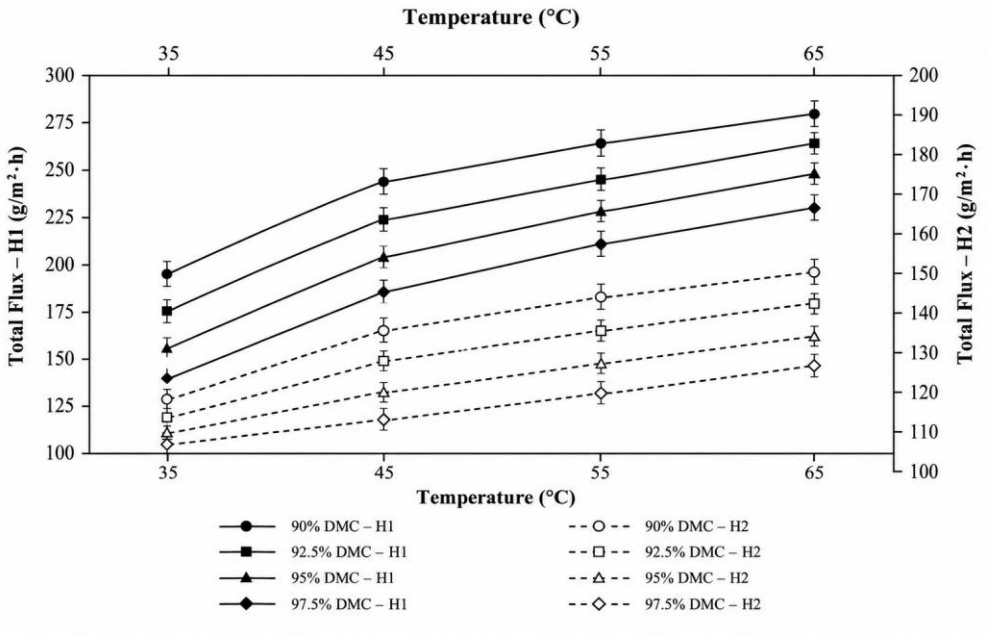

Fig. 7. Total Flux versus Temperature of composite membranes at different temperatures

Figure 7 compares the total permeation flux of the H1 and H2 commercial membranes at operating temperatures of 35–65 °C and DMC feed concentrations of 90–97.5 wt.%. For both membranes, total flux increased with temperature due to enhanced molecular mobility, higher diffusion coefficients, and an increased driving force for permeation. H1 consistently exhibited higher total flux than H2 under all operating conditions, indicating superior permeation performance. The highest flux was obtained with the 90 wt.% DMC feed, while the 97.5 wt.% DMC feed produced the lowest values. This trend is attributed to the higher water content at lower DMC concentrations, which promotes membrane swelling and enhances water sorption and diffusion. As the DMC concentration increased, the reduced water content lowered the driving force for permeation, resulting in decreased flux. The greater temperature dependence of H1 suggests enhanced thermal activation of diffusion compared with H2. Overall, H1 demonstrated superior productivity and is better suited for industrial DMC dehydration.

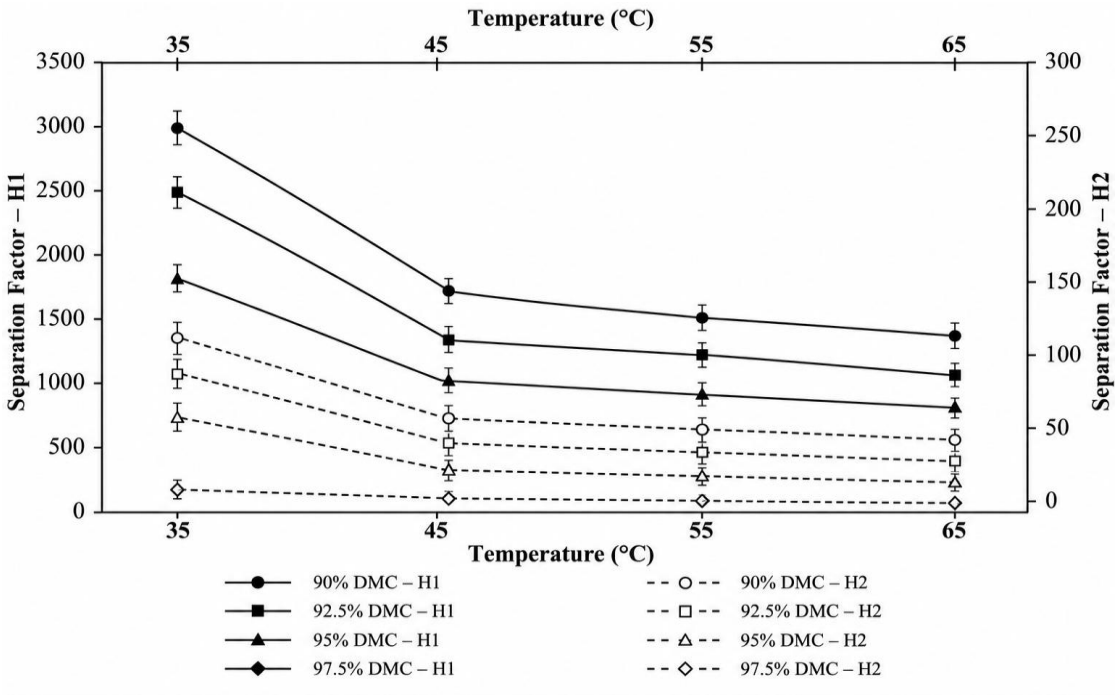

Fig. 8. Separation Factor versus Temperature for PERVAP™ 4100 and Plasma 2540 compositions at different feed compositions

Figure 8 compares the separation factor of the H1 and H2 membranes at operating temperatures ranging from 35 to 65 °C and DMC feed concentrations of 90–97.5 wt.%. H1 consistently exhibited significantly higher separation factors than H2 under all operating conditions, indicating superior water selectivity. This enhanced performance can be attributed to the higher degree of cross-linking of the H1 membrane, which restricts DMC transport while maintaining preferential sorption and diffusion of water molecules through the hydrophilic PVA selective layer. Similar behaviour has been reported for cross-linked PVA membranes, where increased cross-link density improves molecular discrimination and separation efficiency by reducing excessive swelling. For both membranes, the separation factor decreased with increasing temperature and DMC concentration. Elevated temperatures increase polymer chain mobility and enhance the diffusion of both water and DMC, thereby reducing transport selectivity. Likewise, increasing the DMC concentration lowers the water content in the feed, decreasing the driving force for selective water permeation and consequently reducing the separation factor. Although H2 followed the same trend, its lower separation factors indicate lower intrinsic membrane selectivity throughout the investigated conditions. Overall, H1 maintained substantially higher selectivity despite the temperature-induced decline, demonstrating its superior dehydration performance and making it a more suitable membrane for industrial DMC purification requiring high product purity and efficient water removal.

4.2 Component Fluxes and Water/DMC Discrimination

Component flux analysis clearly demonstrates the mechanistic difference between the two membranes. PERVAP™ 4100 exhibited exceptional water selectivity, maintaining water-to-DMC flux ratios ranging from approximately 327:1 at 35°C (90 wt% DMC) to about 67:1 at 65°C, indicating strong suppression of DMC transport while allowing rapid water permeation. In contrast, Plasma 2540 displayed much lower water/DMC flux ratios (approximately 15:1 to 7:1), reflecting significantly greater DMC co-permeation. At the more challenging 97.5 wt% DMC feed, PERVAP™ 4100 limited the DMC flux to only 0.6–3.8 × 10^{-6} kg m^{-2} s^{-1} over the investigated temperature range, whereas Plasma 2540 showed substantially higher DMC fluxes of 12.4–19.4 × 10^{-6} kg m^{-2} s^{-1}. These results confirm that PERVAP™ 4100 achieves high water flux with minimal DMC loss, demonstrating superior water/DMC discrimination compared with Plasma 2540.

Table 3 Water and DMC component fluxes (kg m^{-2} s^{-1} × 10^{-6}) at 90 wt% and 97.5 wt% DMC feed

Feed composition	Temp (°C)	PERVAP™ 4100 (Water/DMC)	Plasma 2540 (Water/DMC)
90 wt% DMC	35	326.8: 1	14.5: 1
	45	150.3: 1	10.5: 1
	55	101.2: 1	8.4: 1
	65	67.0: 1	6.8: 1
97.5 wt% DMC	35	64.2: 1	6.2: 1
	45	39.3: 1	6.0: 1
	55	31.4 : 1	5.4 : 1
	65	24.6 : 1	5.1 : 1

Plasma 2540, in stark contrast, allowed substantial DMC co-permeation at all conditions tested. DMC flux at 90 wt% DMC feed reached 21.70 × 10^{-6} kg m^{-2} s^{-1} at 65°C, yielding a water/DMC flux ratio of only ~7:1. At 97.5 wt% DMC, Plasma 2540 allowed over three times more DMC to permeate than PERVAP™ 4100, representing a significant product loss and contamination concern in an industrial dehydration context [10,22], echoing the general challenge of achieving sharp DMC selectivity that has motivated recent membrane-based DMC/methanol separation strategies such as superwetting membranes [8]. Table 3 compares the water (J_v) and DMC (J^{DMc}) component fluxes of the pristine PERVAP™ 4100 and Plasma 2540-treated membranes at 90 wt.% and 97.5 wt.% DMC feed compositions. Water flux increased with temperature for both membranes, reflecting enhanced molecular diffusion at elevated temperatures. At 90 wt.% DMC, the PERVAP™ 4100 membrane exhibited substantially higher water flux and lower DMC flux than the plasma-treated membrane, indicating superior water selectivity. At 97.5 wt.% DMC, both water and DMC fluxes increased with temperature; however, Plasma 2540 membrane showed higher DMC permeation, whereas the pristine membrane maintained better dehydration performance and overall separation efficiency.

4.3 Water Permeability, Membrane Selectivity, and PSI

Figure 9 compares the water permeability () of the H1 and H2 membranes as a function of feed water concentration at different operating temperatures. For both membranes, water permeability increased markedly with increasing temperature but decreased as the feed water concentration declined from 10 to 2.5 wt.%. Higher temperatures enhance polymer chain mobility and increase the diffusion coefficient of water molecules, thereby facilitating faster transport through the hydrophilic PVA selective layer. Conversely, lower feed water concentrations reduce water sorption within the membrane and diminish the driving force for permeation, resulting in lower permeability. Similar temperature- and concentration-dependent behaviour has been reported for commercial PVA-based pervaporation membranes, where water transport is governed by the combined effects of sorption and diffusion. Throughout the investigated conditions, the H2 membrane exhibited substantially higher water permeability than H1, indicating a less cross-linked and more hydrophilic selective layer that promotes water transport. However, the higher permeability of H2 should be considered together with its lower separation factor, whereas H1 provides a better permeability-selectivity balance for efficient industrial DMC dehydration. Pw

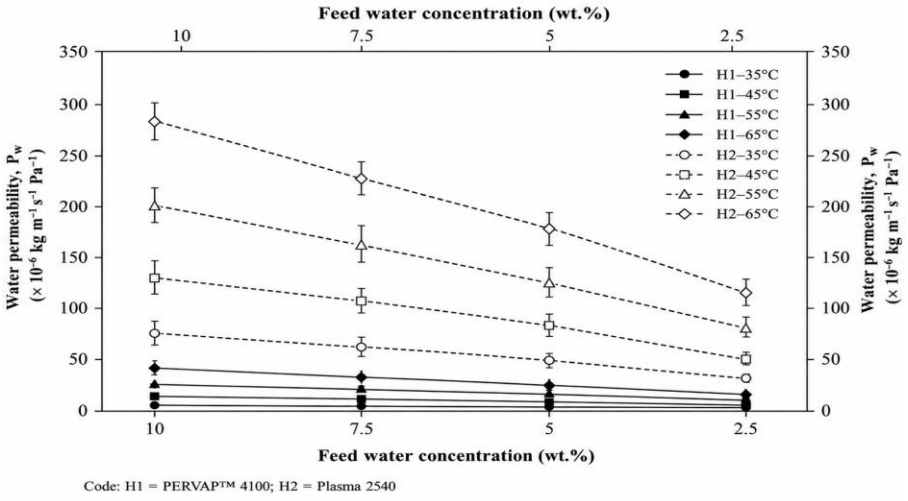

Fig. 9. Effect of feed water concentration on water permeability (P_v) of H1 (PERVAP™ 4100) and H2 (Plasma 2540) membranes at 35, 45, 55, and 65 °C

4.4 Activation Energy of Permeation

Activation energy analysis provides mechanistic insight into the temperature dependence of permeation. PERVAP™ 4100 exhibited consistently higher activation energies for water permeation (22.0 - 29.8 kJ/mol) compared to Plasma 2540 (12.6 - 17.4 kJ/mol). Higher Ep values reflect the greater energy barrier that water molecules must overcome to diffuse through the tighter, more cross-linked PERVAP™ 4100 matrix. This is consistent with the stronger flux-temperature response observed for PERVAP™ 4100 the higher activation energy means that each degree of temperature increase yields a proportionally larger fractional increase in diffusivity, explaining the steeper flux-temperature slope.

For DMC, activation energies were markedly higher than for water in both membranes (38.4 - 47.3 kJ/mol for PERVAP™ 4100 vs. 21.4 - 28.6 kJ/mol for Plasma 2540). The much larger Ep(DMC)/Ep(water) ratio for PERVAP™ 4100 (approximately 1.59) compared to Plasma 2540 (approximately 1.64) indicates that PERVAP™ 4100's dense network is substantially more effective at discriminating DMC transport relative to water, both thermodynamically and kinetically. These activation energy values are in good agreement with those reported for cross-linked PVA systems in the literature [21,30].

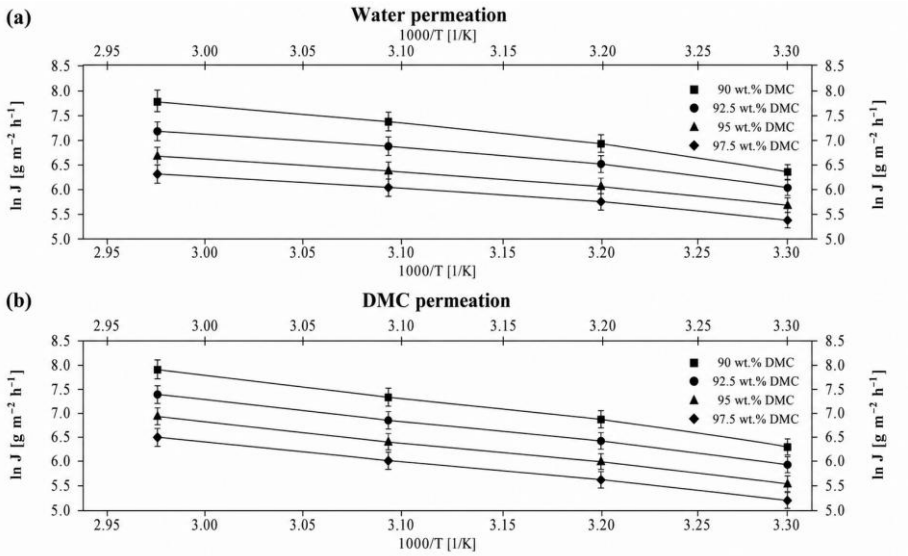

Fig. 10 Arrhenius plots of ln(P_v) versus 1000/T for the Plasma 2540 membrane at different feed DMC concentrations (90, 92.5, 95, and 97.5 wt.% DMC)

Figure 10 presents the Arrhenius plots of (a) water permeation and (b) DMC permeation for the investigated feed compositions. For both components, a linear relationship between ln(J) and 1000/T was obtained, confirming that permeation follows the Arrhenius equation over the studied temperature range. The increase in permeation flux with temperature is attributed to enhanced molecular mobility, increased free volume within the PVA selective layer, and faster diffusion through the membrane. Similar linear Arrhenius behaviour has been reported for commercial PVA-based pervaporation membranes, indicating that permeation is a thermally activated diffusion process. At all temperatures, the 90 wt.% DMC feed exhibited the highest permeation flux, whereas the 97.5 wt.% DMC feed showed the lowest values for both water and DMC. This behaviour reflects the higher water availability and stronger sorption at lower DMC concentrations, which facilitate mass transport. Similar type of results is obtained [41-43]. The linearity of the plots further indicates a consistent transport mechanism without significant structural changes in the membrane throughout the investigated operating conditions. Table 4 compares the activation energies of water and DMC permeation for the H1 and H2 membranes. In both membranes, the activation energy of DMC was higher than that of water, indicating that water permeates more readily through the hydrophilic PVA selective layer. Similar behaviour has been reported for commercial PVA membranes [22, 44, 14], where water transport requires lower energy than organic solvent transport. H1 exhibited higher activation energies for both water and DMC than H2, suggesting a more highly cross-linked structure that provides greater resistance to molecular diffusion. However, the similar ratios indicate comparable transport mechanisms, with H1 & H2 exhibiting better selectivity for efficient water and DMC dehydration from DMC-Water industrial effluent. $Ep,DMC/Ep,Water$

Table 4 - Activation Energy of Water and DMC Permeation for H1 and H2 Membranes

Membrane	Water, Ep (kJ mol^{-1})	DMC, Ep (kJ mol^{-1})	Ep,DMC/Ep,Water
H1	26.1 ± 3.2	43.0 ± 3.8	1.65
H2	15.1 ± 1.9	25.2 ± 2.9	1.67

5. INDUSTRIAL APPLICATION CYCLE 2 DMC DEHYDRATION

The context of the Cycle 2 industrial DMC recovery process defines a demanding and specific separation target. The feed streams the product of a distillation-based DMC recovery column contains approximately 93 wt% DMC, less than 5 wt% water, and approximately 2 wt% other organic impurities. The target product specification is greater than 99 wt% DMC and less than 1 wt% water. The pervaporation membrane must therefore deliver high water selectivity in the 92.5 - 97.5 wt% DMC concentration range, at operating temperatures compatible with industrial thermal utilities (typically 40 - 65°C). Based on the comprehensive performance and characterization data presented in this study, PERVAP™ 4100 is decisively superior for this application. At the representative industrial operating point of 92.5 wt% DMC and 55°C, PERVAP™ 4100 delivered a total flux of 288.18 × 10^{-6} kg m^{-2} s^{-1}, a separation factor of 643.53, and a PSI of 185,161 compared to 145.40 × 10^{-6}, 49.78, and 7,092, respectively, for Plasma 2540. These differences translate directly into significantly reduced membrane area requirements and a higher-purity retentate product with PERVAP™ 4100. The superior mechanical strength and thermal stability of PERVAP™ 4100 further support its selection for continuous industrial operation, where membrane longevity and resistance to creep under sustained vacuum are economically critical. Plasma 2540, while offering lower capital cost and higher intrinsic water permeability, does not meet the selectivity requirements for a single-stage dehydration to the ≤ 1 wt% water specification at feed DMC concentrations above 95 wt%. It could, however, serve a practical role in a preliminary bulk dehydration stage where the water content is high (> 10 wt%), processing speed is prioritized, and a second polishing stage with PERVAP™ 4100 is employed downstream [10,26]. This staged configuration mirrors the broader industrial strategy of coupling pervaporation with conventional distillation in hybrid process arrangements, which have repeatedly been shown to reduce overall energy consumption and capital cost relative to stand-alone azeotropic distillation [45 - 49].

6. CONCLUSIONS

The results show that pervaporation is an effective route for the dehydration of industrial DMC streams, with PERVAP® 4100 giving the highest selectivity and Plasma 2540 showing higher water permeability. Overall, the study provides practical guidance for selecting commercial membranes for efficient and sustainable DMC purification. The principal conclusions are as follows:

1. PERVAP™ 4100 exhibited significantly higher dehydration selectivity than Plasma 2540, achieving a maximum separation factor of 2852 compared with 132.85 for Plasma 2540 under comparable operating

conditions. The superior separation performance is attributed to its denser cross-linked PVA selective layer and enhanced exclusion of DMC molecules.

2. Plasma 2540 demonstrated higher water permeability and permeation flux than PERVAP™ 4100, with maximum water permeability values reaching approximately 1.64×10^{-12} barrer. The higher permeability is associated with its relatively lower cross-linking density and greater membrane swelling, although this was accompanied by substantially lower water/DMC selectivity.
3. Swelling experiments revealed superior dimensional stability for PERVAP™ 4100 throughout the investigated DMC/water compositions. The lower swelling tendency confirms the presence of a more tightly cross-linked polymer network, which contributes to its enhanced separation performance.
4. The activation energy of water permeation was higher for PERVAP™ 4100 than for Plasma 2540, indicating a greater diffusional resistance within the denser membrane structure. This finding is consistent with the observed permeability–selectivity trade-off between the two commercial membranes.
5. FTIR and contact-angle analyses confirmed the structural differences between the membranes. PERVAP™ 4100 exhibited stronger cross-linking-related C–O–C absorption bands and lower membrane swelling, whereas Plasma 2540 and PERVAP™ 4100 displayed equivalent hydrophilicity and higher water permeability. These characterization results were in good agreement with the pervaporation performance data.
6. Mechanical characterization demonstrated superior mechanical strength and durability for PERVAP™ 4100, including higher tensile strength, elongation at break, and overall structural integrity, making it more suitable for long-term industrial operation under vacuum conditions.
7. For the targeted Cycle 2 DMC dehydration process (≥99 wt.% DMC and ≤1 wt.% water), PERVAP™ 4100 is the preferred membrane owing to its exceptional separation efficiency and operational stability. Plasma 2540 may be considered for applications where high permeability is prioritized or as a potential first-stage membrane in multi-stage dehydration configurations.

Overall, the study demonstrates that membrane structure, cross-linking density, swelling behaviour, and transport characteristics collectively govern dehydration performance. The results provide practical guidance for membrane selection in industrial DMC recovery and purification processes.

ACKNOWLEDGMENT

The authors gratefully acknowledge the support provided by the Department of Chemical Engineering, Shroff Rotary institute of Technology, UPL University and CVM University, Gujarat India, for facilitating this research work. The authors thank the laboratory staff of the above-mentioned University for their assistance in membrane fabrication and experimental analysis. No external funding was received for this study. The authors also acknowledge the use of institutional facilities for material characterization and pervaporation experiments. The authors declare that there are no conflicts of interest regarding the publication of this paper.

Author Contributions

Conceptualization, Investigation, Writing- Original Draft, AM; Methodology and Supervision: SRP; Project Administration, Resources: HD, Project Administration, Visualization, KN, all authors have read and agreed to the published version of the manuscript.

Conflict of Interest/Disclosure of Interest Statement

There is “No” potential conflict of interest was reported by the author(s).

Funding

This work not received any specific grant from funding agencies in the public, commercial, or not-for-profit sectors.

Data Availability All data analysed and generated during this are included in this article.

NOMENCLATURE

Symbol	Description	Unit
(A)	Effective membrane area	m^2

(D_w)	Water diffusivity	$m^2\ s^{-1}$
(E_p)	Activation energy of permeation	$J\ mol^{-1}$
(J)	Total permeation flux	$kg\ m^{-2}\ s^{-1}$
(J_i)	Flux of component (i)	$kg\ m^{-2}\ s^{-1}$
(J_w)	Water flux	$kg\ m^{-2}\ s^{-1}$
(J_0)	Pre-exponential factor	$kg\ m^{-2}\ s^{-1}$
(l)	Selective layer thickness	m
(m)	Total permeate mass	kg
(m_i)	Mass of component (i) in permeate	kg
(P_w)	Water permeability	Barrer
$(P_{\{DMC\}})$	DMC permeability	Barrer
$(p_{\{i,sat\}})$	Saturated vapour pressure of component (i)	Pa
(p_p)	Permeate pressure	Pa
(PSI)	Pervaporation Separation Index	-
(R)	Universal gas constant	$8.314\ J\ mol^{-1}\ K^{-1}$
(t)	Collection time	s
(T)	Absolute temperature	K
(X_i)	Weight fraction of component (i) in feed	-
(Y_i)	Weight fraction of component (i) in permeate	-
(α)	Separation factor	-
$(\alpha_{\{mem\}})$	Membrane selectivity	-
(γ_i)	Activity coefficient	-
(ΔC)	Concentration difference across membrane	$kg\ m^{-3}$

References

1. Tamboli, A.H., Chaugule, A.A., Kim, H. (2017). Catalytic developments in the direct dimethyl carbonate synthesis from carbon dioxide and methanol. Chemical Engineering Journal, 323, 530 - 544.
2. Tundo, P., Selva, M. (2002). The chemistry of dimethyl carbonate. Accounts of Chemical Research, 35(9), 706 - 716.
3. Wang, D., Shi, F., Wang, L. (2024). A Review of Catalysts for Synthesis of Dimethyl Carbonate. Catalysts, 14(4), 259.
4. Wei, M.G., Li, H.R., He, L.N. (2024). Synthesis of Dimethyl Carbonate via Transesterification of Ethylene Carbonate and Methanol over Mesoporous KF-loaded Mg-Fe Oxides. ChemPlusChem, 89(7).
5. Kumar, P., Srivastava, V.C., Mishra, I.M. (2016). Dimethyl carbonate synthesis by transesterification of propylene carbonate with methanol: Comparative assessment of Ce-M (M = Co, Fe, Cu and Zn) catalysts. Renewable Energy, 88, 457 - 464.

6. Yan, M., Shen, Y., Wang, S., Zhu, Z., Cui, P., Wang, Y. (2024). Green separation of azeotropes in dimethyl carbonate synthesis by transesterification. Renewable and Sustainable Energy Reviews, 202, 114687.
7. Kumar, N., Srivastava, V.C. (2021). Dimethyl carbonate production via transesterification reaction using nitrogen functionalized graphene oxide nanosheets. Renewable Energy, 175, 1 - 13.
8. Horsley, L.H., Tamplin, W.S. (1952). Azeotropic Data. American Chemical Society, Washington, DC.
9. Kang, C.H., Lin, Y.F., Huang, Y.S., Tung, K.L., Chang, K.S., Chen, J.T., Hung, W.S., Lee, K.R., Lai, J.Y. (2014). Synthesis of ZIF-7/chitosan mixed-matrix membranes with improved separation performance of water/ethanol mixtures. Journal of Membrane Science, 466, 187 - 196.
10. Paul, D.R., Yampol'skii, Y.P. (Eds.) (1994). Polymeric Gas Separation Membranes. CRC Press, Boca Raton.
11. Wijmans, J.G., Baker, R.W. (1995). The solution-diffusion model: A review. Journal of Membrane Science, 107(1 - 2), 1 - 21.
12. Bolto, B., Tran, T., Hoang, M., Xie, Z. (2009). Crosslinked poly(vinyl alcohol) membranes. Progress in Polymer Science, 34(9), 969 - 981.
13. Nguyen, Q.T., Sublet, J., Langevin, D., Chappey, C., Métayer, M., Marais, S. (2011). CO2 permeation through cellulose acetate membranes: Coupling experiment and modeling. Annales de Chimie - Science des Matériaux, 36(4 - 5), 205 - 214.
14. Yeang, Q.W., Zein, S.H.S., Sulong, A.B., Tan, S.H. (2015). Comparison of the pervaporation performance of various carbon nanotube-based nanocomposite membranes in the dehydration of acetone - water and methanol - water systems. Separation and Purification Technology, 127, 252 - 263.
15. Chapman, P.D., Oliveira, T., Livingston, A.G., Li, K. (2008). Membranes for the dehydration of solvents by pervaporation. Journal of Membrane Science, 318(1 - 2), 5 - 37.
16. Huang, R.Y.M. (1991). Pervaporation Membrane Separation Processes. Elsevier, Amsterdam.
17. Yeom, C.K., Lee, K.H. (1996). Pervaporation separation of water - acetic acid mixtures through poly(vinyl alcohol) membranes crosslinked with glutaraldehyde. Journal of Membrane Science, 109(2), 257 - 265.
18. Huang, R.Y.M., Yeom, C.K. (1991). Pervaporation separation of aqueous mixtures using crosslinked poly(vinyl alcohol) (PVA). II. Permeation of ethanol - water mixtures. Journal of Membrane Science, 58(1), 33 - 47.
19. Won, W., Feng, X., Lawless, D. (2003). Pervaporation with chitosan membranes: Separation of dimethyl carbonate/methanol/water mixtures. Separation and Purification Technology, 31(2), 129 - 140.
20. Dogan, H., Hilmioglu, N.D. (2010). Dissolution of chitosan and casting of composite membranes for pervaporation. Chemical Engineering Journal, 160(1), 39 - 47.
21. Tang, X.H., Wang, Z., Feng, X., Wang, C.B., Zhu, M. (2020). Hybrid PVA - silica membranes for dehydration of dimethyl carbonate: Effect of silica loading and cross-linking. Separation and Purification Technology, 234, 116067.
22. Neel, J. (1991). Introduction to pervaporation. In: Huang, R.Y.M. (Ed.), Pervaporation Membrane Separation Processes. Elsevier, Amsterdam, pp. 1 - 64.
23. Panda, S. R., Mukherjee, M., & De, S. (2014). Adsorptive removal of humic acids and microbes by polyacrylonitrile–chitosan composite membrane. Presented at the AIChE Annual Meeting, Atlanta, Georgia, USA.
24. Liu, G., Hou, D., Wei, W., Xiangli, F., Jin, W. (2005). Pervaporation separation of butanol - water mixtures using polydimethylsiloxane/ceramic composite membrane. Chinese Journal of Chemical Engineering, 19(1), 40 - 44.
25. Panda, S. R., Mondal, M., & De, S. (2016). Hollow fiber NF membranes involving $ZnCl_2$ incorporated polysulfone (PSF)/polyethylene glycol. Indian Patent No. 348184.
26. Gao, Z., Yue, Y., Li, W. (2012). Ultrathin zeolite X membranes for pervaporation dehydration of ethanol. Journal of Membrane Science, 415 - 416, 729 - 735.
27. Gupta, O., Roy, S., Rao, L., Mitra, S. (2022). Graphene Oxide-Carbon Nanotube (GO-CNT) Hybrid Mixed Matrix Membrane for Pervaporative Dehydration of Ethanol. Membranes, 12(12), 1227.
28. Kuzminova, A., Dmitrenko, M., Zolotarev, A., Myznikov, D., Selyutin, A., Su, R., Penkova, A. (2022). Pervaporation Polyvinyl Alcohol Membranes Modified with Zr-Based Metal Organic Frameworks for Isopropanol Dehydration. Membranes, 12(10), 908.
29. Dinda, S., Patwardhan, A. V., Panda, S. R., & Pradhan, N. C. (2008). Kinetics of reactive absorption of carbon dioxide with solutions of aniline in carbon tetrachloride and chloroform. Chemical Engineering Journal, 136(2–3), 349–357.
30. Amnuaypanich, S., Patthana, J., Phinyocheep, P. (2009). Mixed matrix membranes prepared from natural rubber/polyvinyl alcohol semi-interpenetrating polymer network (NR/PVA semi-IPN) incorporated with zeolite 4A for the pervaporation dehydration of water - ethanol mixtures. Chemical Engineering Science, 64(23), 4908 - 4918.
31. Tsai, H.A., Li, L.D., Lee, K.R., Wang, Y.C., Li, C.L., Huang, J., Lai, J.Y. (2010). Effect of surfactant addition on the morphology and pervaporation performance of asymmetric polysulfone membranes. Journal of Membrane Science, 176(1), 97 - 103.
32. Svang-Ariyaskul, A., Huang, R.Y.M., Douglas, P.L., Pal, R., Feng, X., Chen, P., Liu, L. (2006). Blended chitosan and polyvinyl alcohol membranes for the pervaporation dehydration of isopropanol. Journal of Membrane Science, 280(1 - 2), 815 - 823.
33. DeltaMem AG (Switzerland). Product Specification: PERVAP™ 4100 Membrane. Technical Datasheet (current edition).
34. Shivohm Membrane Systems (2023). Plasma 2540 Membrane - Technical Specification. Sangli, Maharashtra, India.

35. Mansur, H.S., Sadahira, C.M., Souza, A.N., Mansur, A.A.P. (2008). FTIR spectroscopy characterization of poly(vinyl alcohol) hydrogel with different hydrolysis degree and chemically crosslinked with glutaraldehyde. Materials Science and Engineering: C, 28(4), 539 - 548.
36. Awada, H., Daneault, C. (2015). Acid catalysed cross-linking of poly(vinyl alcohol) (PVA) by glutaraldehyde: effect of crosslink density on the characteristics of PVA membranes used in microbial fuel cells. RSC Advances, 5, 78603 - 78609.
37. Panda, S. R., & De, S. (2015). Performance evaluation of two-stage nanofiltration for treatment of textile effluent containing reactive dyes. Journal of Environmental Chemical Engineering, 3(3), 1678–1690.
38. Arif, Z., Sethy, N.K., Mishra, P.K., Kumar, P. (2018). Investigating the influence of sol-gel derived PVA/SiO2 nanocomposite membrane on pervaporation separation of azeotropic mixture I. Effect of operating condition. Journal of Porous Materials, 25, 1203 - 1211.
39. Xie, Z., Hoang, M., Duong, T., Ng, D., Dao, B., Gray, S. (2011). Sol-gel derived poly(vinyl alcohol)/maleic acid/silica hybrid membrane for desalination by pervaporation. Journal of Membrane Science, 383(1 - 2), 96 - 103.
40. Lipnizki, F., Field, R.W., Ten, P.K. (1999). Pervaporation-based hybrid process: A review of process design, applications and economics. Journal of Membrane Science, 153(2), 183 - 210.
41. Van Hoof, V., Van den Abeele, L., Buekenhoudt, A., Dotremont, C., Leysen, R. (2004). Economic comparison between azeotropic distillation and different hybrid systems combining distillation with pervaporation for the dehydration of isopropanol. Separation and Purification Technology, 37(1), 33 - 49.
42. Panda, S. R., De, S., & Mukherjee, M. (2016). Chitosan-coated iron oxide–polyacrylonitrile mixed matrix membrane for removal of humic acid. Indian Patent No. 319460.
43. Giles, N.F., Wilson, G.M. (2000). Phase equilibria on seven binary mixtures. Journal of Chemical and Engineering Data, 45(1), 146 - 153.
44. Huang, Z., Guan, H., Tan, W.L., Qiao, X., Kulprathipanja, S. (2006). Pervaporation study of aqueous isopropyl alcohol solution through zeolite-incorporated multilayer poly(vinyl alcohol) membranes: Effect of zeolites. Journal of Membrane Science, 276(1 - 2), 260 - 271.
45. Panda, S. R., & De, S. (2013). Role of polyethylene glycol with different solvents for tailor-made polysulfone membranes. Journal of Polymer Research, 20(7), 179.
46. Panda, S. R., Mukherjee, M., & De, S. (2015). Preparation, characterization and humic acid removal capacity of chitosan-coated iron oxide/polyacrylonitrile mixed matrix membrane. Journal of Water Process Engineering, 6, 93–104.
47. Nickel, G., Bücking, M., Heitz, M. (2003). PVA/PAN composite membranes for organic solvent dehydration. Journal of Membrane Science, 216, 191 - 202.
48. Park, H.C., Meertens, R.M., Mulder, M.H.V., Smolders, C.A. (2001). Pervaporation of alcohol - water mixtures through zeolite-filled PDMS membranes. Industrial & Engineering Chemistry Research, 40(23), 5755 - 5763.
49. Madalgi, A. P., Panda, S. R., Dave, H. K., & Nath, K. (2026). Mixed matrix pervaporative membranes for solvent dehydration as a next step to energy intensive distillation. International Journal of Drug Delivery Technology, 16(56S), 1385–1401. https://doi.org/10.25258/ijddt.16.56s.152